sustainability

MDPI

Article

Performance Prediction of Proton Exchange Membrane Fuel Cells (PEMFC) Using Adaptive Neuro Inference System (ANFIS)

Tabbi Wilberforce [1,*] and Abdul Ghani Olabi [2]

[1] Mechanical Engineering and Design, Aston University, School of Engineering and Applied Science, Aston Triangle, Birmingham B4 7ET, UK

[2] Department of Sustainable and Renewable Energy Engineering, University of Sharjah, P.O. Box 27272, Sharjah, UAE; aolabi@sharjah.ac.ae

* Correspondence: Tabbi.Awotwe@uws.ac.uk

Received: 20 May 2020; Accepted: 15 June 2020; Published: 17 June 2020

Abstract: This investigation explored the performance of PEMFC for varying ambient conditions with the aid of an adaptive neuro-fuzzy inference system. The experimental data obtained from the laboratory were initially trained using both the input and output parameters. The model that was trained was then evaluated using an independent variable. The training and testing of the model were then utilized in the prediction of the cell-characteristic performance. The model exhibited a perfect correlation between the predicted and experimental data, and this stipulates that ANFIS can predict characteristic behavior of fuel cell performance with very high accuracy.

Keywords: machine learning; ambient conditions; flow rate; pressure; hydrogen

1. Introduction

As the world continues to strive for alternative energy generation media in order to fight climate change, energy generation sources for electricity production must be critically reviewed [1–3]. Fossil product over the last few years has been the major source of energy generation worldwide [4–7]. The world today considers it a key contributor to carbon emissions into the atmosphere hence the urgent need to consider an alternative [8–10]. Renewable sources are, therefore, perceived as the best replacement for these fossil products [11,12]. Again, fossil product prices are unstable, and the worst part is their harmful effect on the environment. Several research activities today are geared towards the optimization of operational conditions of fuel cells [13].

Fuel cells produce direct current via a chemical reaction between fuel and an oxidant. The conversion method for the fuel cell into electricity is considered as being environmentally friendly and efficient. The ambient conditions surrounding the cell affect its efficiency. It, therefore, becomes very important that a method used to validate these operational parameters is developed [14,15]. These validation methods could be mathematical and numerical models. These models can be used in place of other experimental investigations in other to obtain results for fluid flow, heat transfer, and a chemical reaction.

PEMFCs are one of the types of fuel cells known due to their low operating temperature range but high efficiency [16]. They are usually made up of a membrane electrode assembly which supports electrochemical reactions. A platinum catalyst on the membrane is what speeds up the chemical reaction and potential add up to the overall cost of the cell. PEM fuel cells have fast start up time compared to other types of fuel cells. Again, there are many options in terms of the type of fuel used as a reactant. All these merits are some of the practical reasons why PEM fuel cells are an alternative source of energy generation [17]. The other types of fuel cells are good but ideal for specific

applications and tend to have their individual limitations. Solid oxide being operated at a higher rate are ideal for power plants. Operating the cells at higher temperatures implies a higher cost of operation. Due to accelerated research activities, fuel cells today are being integrated into renewable sources, such as wind and solar energy systems, in order to improve the overall efficiency of the system. The hydrogen needed as fuel, as explained earlier, can be obtained via many processes [18]. Under laboratory conditions, these hydrogen gasses are stored in pressurized gas bottles or produced through an electrolytic process. The best operational conditions that would increase the performance of the cell are directly related to the overall cost of the cell. Several investigations have been conducted from the literature to mathematically predict the performance of fuel cells [19–21]. The main issue regarding these mathematical methods has to do with the accuracy of the results generated because the physical processes used are quite complex. For complex nonlinear conditions, simple computation techniques, like artificial neural network, are often used. Artificial neural networks are developed to be able to learn and generalize in order to generate predicted solutions [20]. From the literature, several investigations have been conducted using prediction statistically and correlation analysis in fuel cells. The relevance of using a predicting model is also dependent on the adoption of a good technique coupled with a strategy to accurately determine the operational conditions that will enhance the overall performance of the cell. The relationship between the experimental data and the predicted data is conducted via correlation analysis. These mathematical models are designed to reduce the cost in carrying out these experimental investigations and also to save time. Investigations can, therefore, be justifiable using these theoretical models compared with conceptualized models. Artificial neural networks are able to predict nonlinear systems, unlike that of the linear regression methods. The output results from artificial neural networks is dependent on the input parameters hence considered to work like the human brain.

The application of an adaptive neuro-fuzzy inference system (ANFIS) could be traced to the 1990s using Takagi–Sugeno fuzzy model [21,22]. This technique has been used in some fuel cell investigations producing very accurate results but not predominant specifically in proton exchange membrane fuel cell analysis. The technique is designed to be a combination of neural networks and theories for the operation of systems using fuzzy logic [17]. The results generated are highly dependent on each concept. As explained earlier, the physical architecture coupled with the information is managed by neural networks while the fuzzy logic is designed to function like the human brain and the management of uncertainties in the system. The feature of a set of data is learnt buy adaptive neuro-fuzzy inference system. The parameters for the system are then made to change to be the same as the error criterion for system for output generation. The training times and the computational power required tend to be less, hence ideal for the prediction of operational parameters for proton exchange membrane fuel cells [23–26].

In a nutshell, this investigation is aimed at exploring the best operational parameters that would yield the maximum performance from a proton exchange membrane fuel cell. The application of an adaptive neuro-fuzzy inference system in predicting the current and voltage obtained from an experimental investigation would be ascertained [27–30]. The accuracy of the results will be dependent on a comparison of the results between the root mean squared error (RMSE) criterion, the coefficient of correlation and the coefficient of determination. With the aid of multiple linear regression, as well as feed-forward back propagation neural network, a comparative study will be conducted to clearly show the accuracy of results generated using an adaptive neuro-fuzzy inference system.

2. Experimental Analysis

2.1. Fuel Cell Testing Procedure

Fuel cells obtained from fuel cell store United States with an active area of 11.46 cm^2 was used in this investigation. The bipolar plate channel designs were serpentine, and according to the manufacturer's specifications, the membrane for these types of fuel cells had to be well humidified to reduce any form

of resistance on the membrane. The operating parameters used in the investigation are depicted in Table 1.

Table 1. Testing of fuel cell operational parameters.

Level of numerical design	−1	+1
Input variable level	Minimum	Maximum
H_2 pressure	1 bar	2.5 bar
O_2 pressure	0.8 bar	2.3 bar
H_2 flow rates	15 mL/min	150 mL/min
O_2 flow rates	15 mL/min	150 mL/min

Table 2 captures the materials used for the fuel cell components and the loading conditions for the catalyst (platinum).

Table 2. Fuel cell material composition.

Fuel Cell Component	Material	Characteristics
Housing	Acetyl	Supplier: (Fuel Cell Store)
Membrane electrode assembly	Nafion 212	Active area: 3.4 × 3.4 cm Catalyst loading 0.4 mg/cm^2 Pt/c.0.55 g cm^3 bulk
Bipolar plate	Graphite	Supplier: Fuel cell store 24 pores/cm Thickness: 0.65 mm
Sealing	Silicon	Supplier: Fuel Cell Store Thickness: 0.8 mm Supplier: Fuel Cell Store

2.2. Experimental Set-Up

The components used in the experiments are captured in Figure 1. Production of hydrogen for the fuel cell was carried out using a hydrogen generator from Peak Scientific, UK. The oxygen for the electrochemical reaction was also obtained from the air because our fuel cell is air-breathing. A fan helped speed up the circulation of air and mass transport. The hydrogen flow rate was also measured using a flow meter before making its way into the fuel cell. From the determination of the hydrogen flow rate, the next step was to pass the gas through a humidification chamber. This allows the dried hydrogen gas to pick up some water molecules for the humidification of the membrane. The experimental working environment had a relative humidity of 0.74. The airflow rate was determined from the data sheet of the fan used in the investigation. A potentiostat was utilized for the generation of the iv-curve for each operating condition. The open circuit voltage and the current were all deduced using a multi-meter. A thermocouple attached to the cell-supported the determination of cell operating temperature at varying conditions. The cell was operated between temperatures of 50 °C and 60 °C.

2.3. Adaptive Neuro-Fuzzy Inference System (ANFIS)

The development of an adaptive neuro-fuzzy inference system can be traced to the 1990s. It was designed as software made of a combination of neural network and fuzzy logic. The input and output datasets are learned in artificial neural network for the generation of accurate results. Fuzzy logic interprets, organizes, and also adds an element of rationalization to data. There are four compositions of the fuzzy inference system, namely fuzzifier, fuzzy rules, defuzzifier, and inference engine. The output for a fuzzy inference system is known via the building of the fuzzy rules, the inputs being fuzzified with the aid of functions, building a rule strength and determining its consequence. A distribution for

the output is generated via the combination of these consequences. The Sugeno and Mamdani are the well-known models of fuzzy inference system. The application of the fuzzy rules being connected to the fuzzy set and further defuzzified is classified under the Mamdani model. The Sugeno fuzzy inference system functions just like the Mamdani type. The only difference between the two is the fact that there is no output function added to the system for the Sugeno fuzzy inference system. Combining artificial neural network and fuzzy inference system uses the same learning techniques in neural network and also adopts the integration of fuzzy reasoning to add logic and the prior knowledge effect. Learning of the membership function for the fuzzy logic is done using artificial neural network. This technique supports the building of the input data for the model as fuzzy IF—THEN rules in the FIS. This process is conducted for the optimization of the parameters utilized in the development of the fuzzy inference system with an application to ensure the data are learned. An adaptive neuro-fuzzy inference system is designed to have two inputs and the number of layers being five, as depicted in Figure 1. The adaptive nodes and nodes are shown in the square and circles in Figure 2.

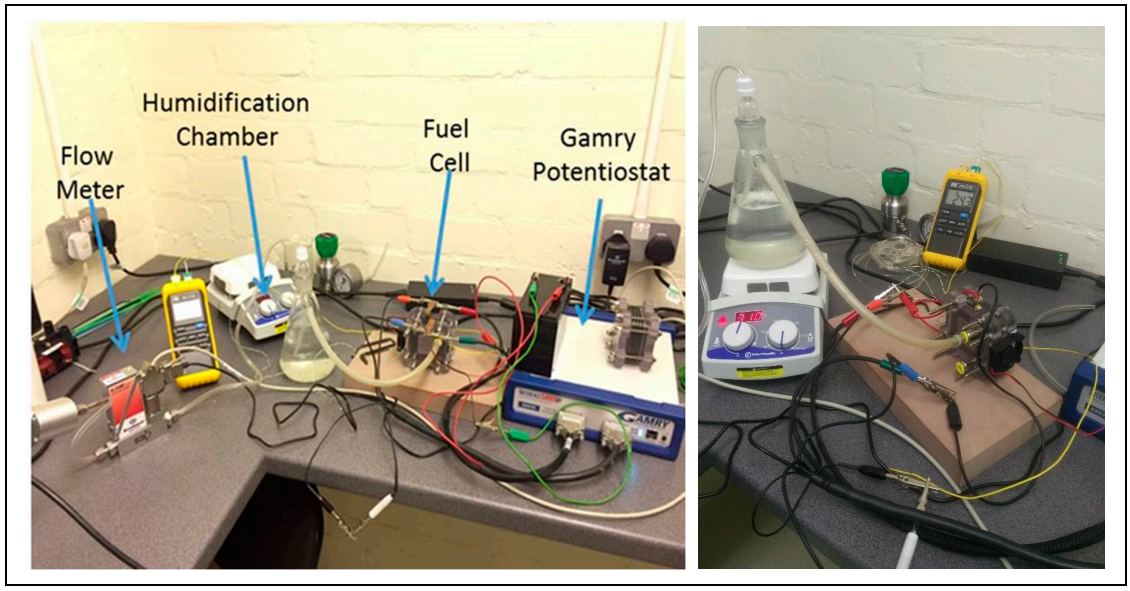

Figure 1. Fuel cell experimental set up.

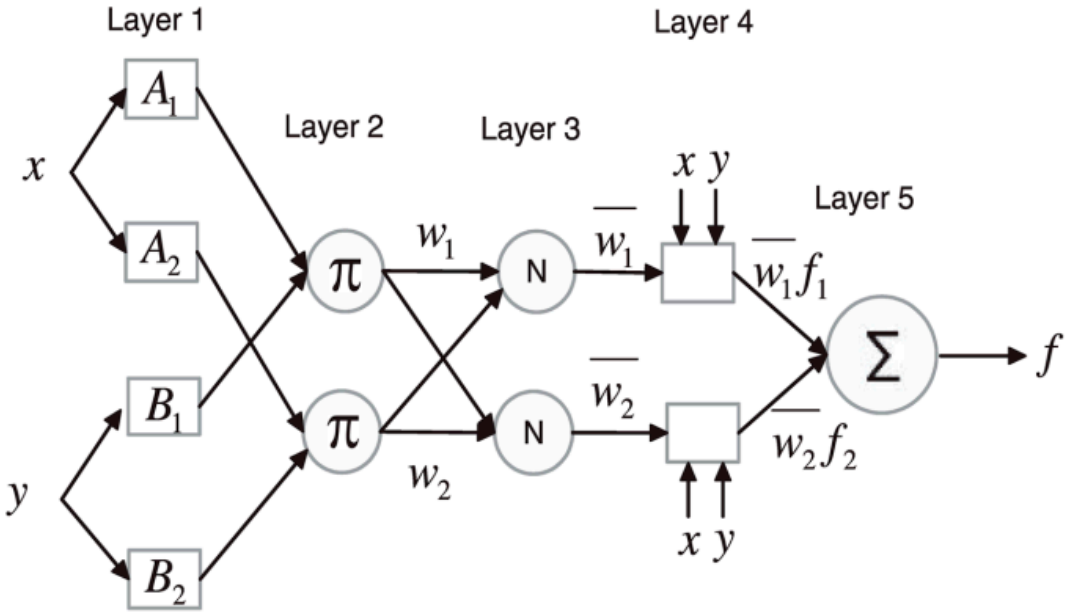

Figure 2. Structure of adaptive neuro-fuzzy inference system.

There are apparently four adaptive nodes for the parameters denoted as A_1, A_2, B_1, B_2. Mathematical representation for the fuzzy IF—THEN rules is shown in Equations (1) and (2). Rule 1: If x is A_1 and y is B_1, then

$$f_1 = p_1x + q_1y + r_1 \tag{1}$$

Rule 2: If x is A_2 and y is B_2, then

$$f_2 = p_2x + q_2y + r_2 \tag{2}$$

The consequent parameters are also captured as p_i, q_i, r_i where $i = 1, 2$. From the structure of the adaptive neuro-fuzzy inference system, x and y can be found in layer 1 representing the input variables. They are then transformed to a membership figure with the aid of membership functions. The generalized bell functions are the common membership functions used in an adaptive neuro-fuzzy inference system. The value representing the fuzzy membership, which also doubles as layer 1 output, is captured as O_i. This value denotes any ith node in layer j. Equations (3) and (4) below represent the adaptive nodes undergoing varying operations.

$$O_{1,i} = \mu A_i(x),\ i = 1, 2 \tag{3}$$

$$O_{1,i} = \mu B_{i-2}(y),\ i = 3, 4 \tag{4}$$

Equations (3) and (4) denote the membership functions, often the generalized bell functions for the fuzzy dataset A_1, A_2, B_1, B_2. The connection between these datasets for the input x and y and the fuzzy set is also captured in Equations (3) and (4). The parameters for the ith node for layer j are captured in the variables A_i and B_{i-2}. The μ function is captured in Equation (5).

$$\mu_{A_i}(x) = \left\{1 + \left[\frac{(x - c_i)}{a_i^2}\right]^{b_i}\right\}^{-1} \tag{5}$$

Equations (6)–(9) represent the membership functions in mathematical connotations.
Triangular:

$$\mu_x(a) = \frac{(a - x)}{(y - x)},\ x \le a \le y = \frac{(z - a)}{(z - y)},\ y \le a \le z = 0 \tag{6}$$

Gaussian:

$$\mu_x(a) = \frac{1}{1 + \left(\frac{a-z}{x}\right)^2} \tag{7}$$

Bell-shaped:

$$\mu_{Xi}(a) = \frac{1}{1 + \left(\frac{a-z_i}{x_i}\right)^{2x_i}},\ i = 1, 2, \ldots \tag{8}$$

$$\mu_{Yi}(b) = \frac{1}{1 + \left(\frac{b-z_j}{x_j}\right)^{2y_j}},\ j = 1, 2, \ldots \tag{9}$$

An alteration of the consequent parameters for the membership functions results in the production of different membership functions and supports flexibility in the definition of membership functions. Layer 2 subsequently is made up of fixed nodes operating on multiplication rules. The product of input signals is developed for the generation of rules for firing strength. The operation is captured in Equation (10).

$$O_{2,i} = \omega_i = \mu_{A_i}(x) \times \mu_{B_i}(x),\ i = 1, 2 \tag{10}$$

Layer 3 ensures the normalization of the firing strength obtained in the second layer. The ratio for the firing strength of the *i*th rule to the sum of rules in the model is determined at this point. An expression for the normalization techniques is captured mathematically in Equation (11).

$$O_{3,i} = \overline{\omega_i} = \frac{\omega_i}{\omega_1 + \omega_2}, \; i = 1, 2 \tag{11}$$

The output computations are obtained in the fourth layer. There is an adjustment of the consequent parameters until an optimized value is generated with the least error. The layer is composed of adaptive nodes that support the calculation of total output for the developed model. The output for layer 3, $\overline{w_i}$, is multiplied by a parameter set $\{a_i, \; b_i, \; c_i\}$ to get the output of layer 4 captured in Equation (12).

$$O_{4,i} = \overline{\omega_i} f_i = \overline{\omega_i}(p_i x + q_i y + r_i) \tag{12}$$

There is finally adding up of all the outputs in layer 4 for the final output of the adaptive neuro-fuzzy inference model. A summation function operation can be found in layer 5 with one fixed node depicted in Equation (13).

$$O_{5,i} = \sum_i \overline{\omega_i} f_i \tag{13}$$

2.4. Multiple Linear Regression (MLR)

The cause–effect correlation between variables for a given dataset aimed at obtaining predicted equations can be executed with the aid of regression analysis. This statistical model can be utilized as well to explain how many variables explanatorily define a variable that is dependent. Multiple linear regression predicts the linear correlation between independent and dependent variables. Multiple linear regression uses a linear equation depicted in Equation (14) for the observation of the data. The dependent variables are usually subject to change hence denoted by the coefficient in Equation (14). This occurs as a result of changes in the independent variable by a unit of one. In an instance where other variables are zero, the constant attached to Equation (14) would represent the dependent variable.

$$y_i = \beta_0 + \beta_1 x_{i1} + \beta_2 x_{i2} + \ldots + \beta_p x_{ip} + \varepsilon \tag{14}$$

where for any $i = n$ observations, the variable that is dependent is denoted as y_i which in this case will be current and voltage whiles the variable that is independent is denoted as x_i. The y—intercepts on the other hand is represented as β_0 and β_p and this is the slope coefficients of the independent variable. Any error obtained as a result of the modeling method is also denoted as ϵ. Evaluation of the degree of linearity is done using the coefficient of determination. The actual and predicted variable difference is accounted for using the error term. To check whether the application of multiple linear regression is ideal for a particular dataset, techniques such as linearity, extreme value coupled with normality is utilized.

2.5. Model Implementation

An adaptive neuro-fuzzy inference system (ANFIS) was used in the estimation of voltage and current at varying reactant (hydrogen and oxygen) pressure and flow rate in proton exchange membrane fuel cell. Due to the convergence rate of the Sugeno approach being very fast, it was utilized in this investigation. Again, the accuracy of the Sugeno method is higher compared to the Mamdani technique. The optimal membership function was also deduced via the trial and error technique. The least root mean squared (RMS) error was selected after using the membership function. The minimum error method was selected considering other variables like the approach for generating the fuzzy inference system, composition function types, and membership functions number in the hidden layer and interference. The data generated from the experimental investigation were separated into training and testing datasets. These datasets were then utilized as input data in MATLAB, specifically in the

neuro-fuzzy designer app. The size of the data and application influenced the structure ideal for the model. The model was then trained after the selection of the important parameters. This step was carried out to ensure the learning ability for the model was viable and also supported the determination of the structural parameters for an algorithm. An integration of gradient descent and the least square technique is the hybrid optimization algorithm. There is forward propagation of the output till it gets to the fourth layer. The least square technique is used for the determination of the consequent parameters. There is further back propagation of the errors attained and alteration of the premise parameters. They are further adjusted with the aid of the gradient descent algorithm. The error factor in the adaptive neuro-fuzzy inference system is depicted in Equation (15).

$$E = \sum_{k=1}^{n} \left(f_k - f_k' \right)^2 \tag{15}$$

The hybrid method uses other algorithms for each of the training parts. The local minima convergence is eliminated and this tends to enhance the model performance as well. The pattern for the test for the neuro-fuzzy app was assessed.

3. Results and Discussion

3.1. Results from Experiment

Polarization curves are used to determine the performance of fuel cells at varying operational conditions. From the experimental data, an increase in the reactant pressure coupled with the flow rate caused an increase in the power density generated for the cell under investigations. This can be attributed to the current generated from the fuel cell being high, as shown in Figure 3.

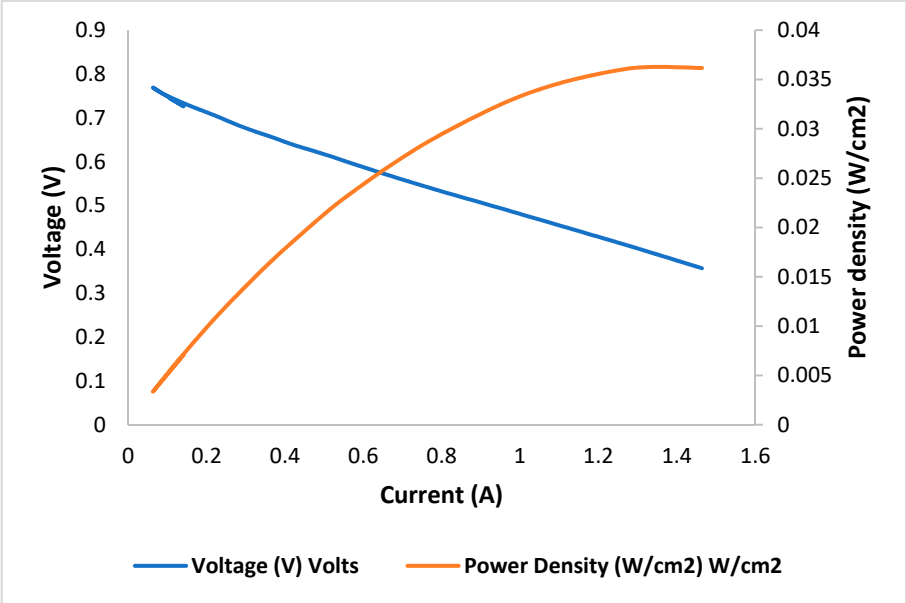

Figure 3. Performance of proton exchange membrane fuel cell at lower pressure and flow rate of the reactant.

Figures 4–6 captures the overall fuel cell performance at varying ambient and cell operating conditions.

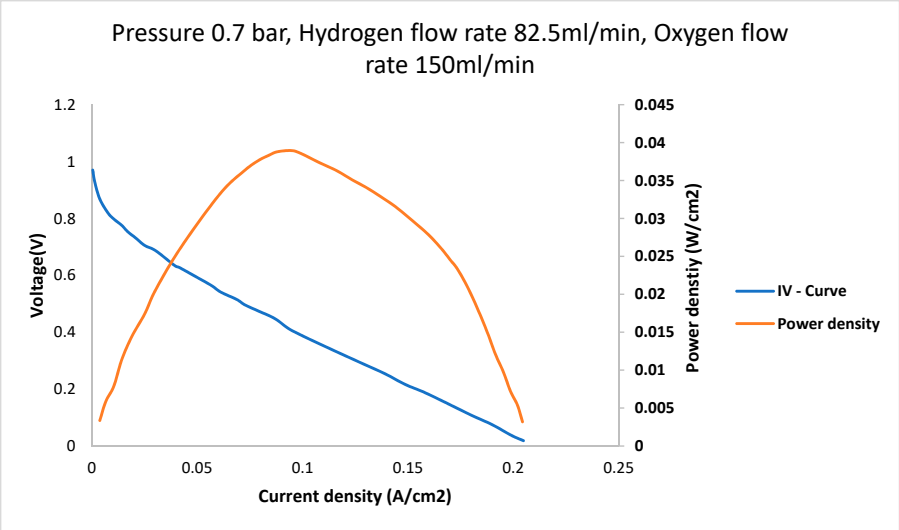

Figure 4. Fuel cell performance at varying low pressure and reactant flow rate.

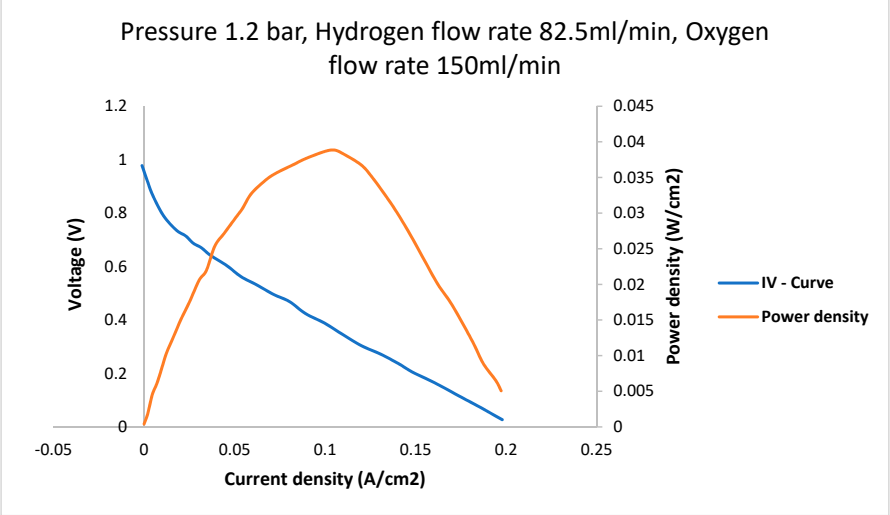

Figure 5. Fuel cell performance at varying low pressure and reactant flow rate.

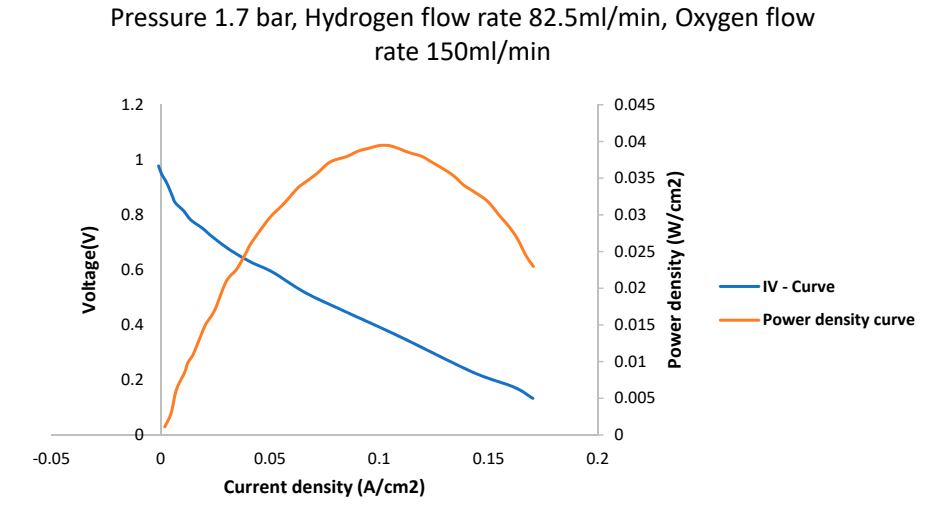

Figure 6. Fuel cell performance at varying low pressure and reactant flow rate.

3.2. Analysis of Experimental Data Using Statistical Technique

Multiple regression analysis involves the determination of regression equation hence the four input parameters: The oxygen flow rate, hydrogen flow rate, oxygen pressure, and the hydrogen pressure were selected as the independent variables while current and voltage were the dependent variables. The statistics for the input parameters are captured in Table 3.

Table 3. Analysis of experimental data statistically.

Data	N	Mean	Standard Deviation	Sum	Minimum	Median	Maximum
Hydrogen Pressure	22	1.71591	0.48975	37.75	1	1.75	2.5
Oxygen Pressure	22	1.51591	0.4316	33.35	0.8	1.55	2.3
Hydrogen flow rate	22	85.56818	48.75187	1882.5	15	82.5	150
Oxygen Flow Rate	22	85.56818	44.07739	1882.5	15	82.5	150
Current	22	0.50955	0.44897	11.21	0.065	0.339	1.464
Voltage	22	0.62314	0.12953	13.709	0.357	0.6645	0.768

Tables 4 and 5 explain the analysis of variance for the current and voltage (dependent variable) at varying flow rate and pressure (input parameters, independent variable). From the table, it can be observed that the independent variable (varying flow rate and pressure) has an enormous influence on the estimation of the dependent variable (current and voltage). From Tables 2 and 3, the F value is 2.06468 and 1.85269.

Table 4. Analysis of variance for current.

	DF	Sum of Squares	Mean Square	F Value	Prob > F
Model	4	1.38408	0.34602	2.06468	0.13053
Error	17	2.84904	0.16759		
Total	21	4.23312			

Table 5. Analysis of variance for voltage.

	DF	Sum of Squares	Mean Square	F Value	Prob > F
Model	4	0.10697	0.02674	1.85269	0.16532
Error	17	0.24538	0.01443		
Total	21	0.35235			

Table 6 summarizes the multiple linear regression model for the current and the voltage. It can be observed that the adjusted R—square value for current is higher compared to voltage. The application of an adaptive neuro-fuzzy inference system will then address all non-linearities in the model.

Table 6. Summary of regression analysis.

Current			Voltage		
Variable	Value	Std. Error	Variable	Value	Std. Error
Constant	1.5481	0.48767	Constant	0.33199	0.14312
Hydrogen Pressure	−0.36593	0.18367	Hydrogen Pressure	0.09843	0.0539
Oxygen Pressure	−0.14583	0.20849	Oxygen Pressure	0.04059	0.06119
Hydrogen flow rate	−0.00336	0.00185	Hydrogen flow rate	9.722×10^{-4}	5.42×10^{-4}
Oxygen Flow Rate	0.00114	0.00204	Oxygen Flow Rate	-2.62×10^{-4}	5.989×10^{-4}
Adjusted R^2		0.1686	Adjusted R^2		0.1397

3.3. Adaptive Neuro-Fuzzy Inference System Results

The investigation used an adaptive neuro-fuzzy inference system to develop a correlation between the flow rate and pressure on current and voltage in a proton exchange membrane fuel cell experiment [31–33]. The experimental data were first trained and later tested [34–39]. The membership function for the model was used via trial and error technique. The hybrid learning algorithm was further used for the training of the process. Figure 7 captures the four input parameters and two membership functions for the input and output. The fuzzy rules are captured in the neutrons in layer 3. Neutrons also captured in layer 3 are the rules and conditions. The model developed had the fuzzy—IF-THEN rules for the membership functions below. The model was trained for a hundred iterations. Table 7 captures the model specification using the adaptive neuro-fuzzy inference system.

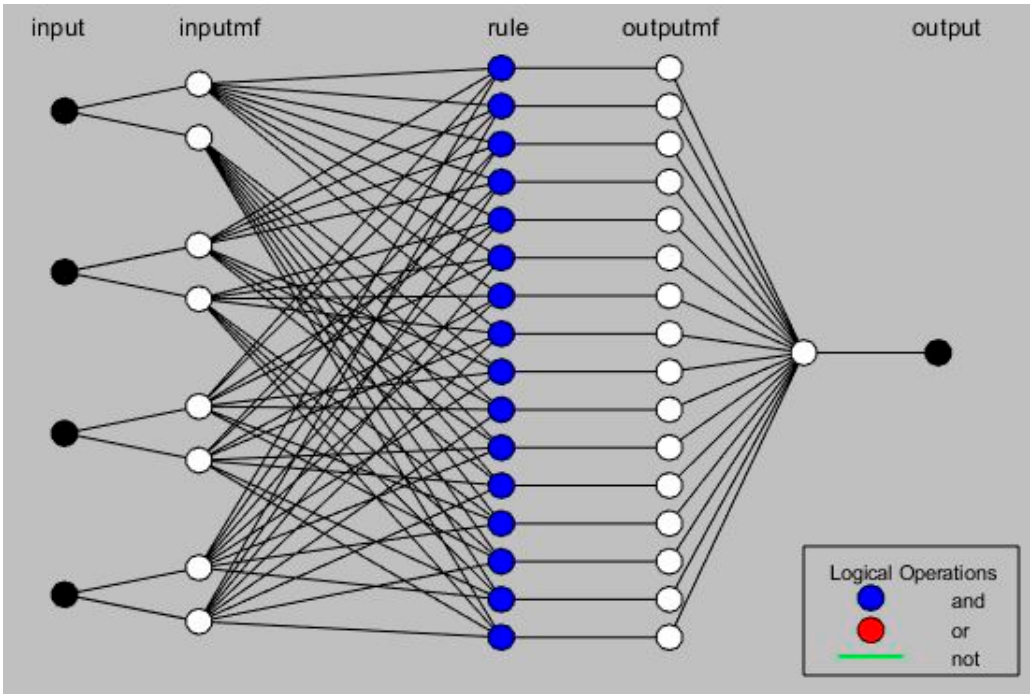

Figure 7. Adaptive neuro-fuzzy inference system structure.

Table 7. Model specification using the adaptive neuro-fuzzy inference system.

Variable	Current	Voltage
	Value	Value
Number of nodes	55	193
Number of linear parameters	80	405
Number of nonlinear parameters	16	24
Total number of parameters	96	429
Number of training data pairs	18	19
Number of checking data pairs	0	0
Number of fuzzy rules	16	16

The experimental data plotted against the predicted for voltage and current using the adaptive neuro-fuzzy inference system captured in Figures 8 and 9 show the results for the training and testing for the current.

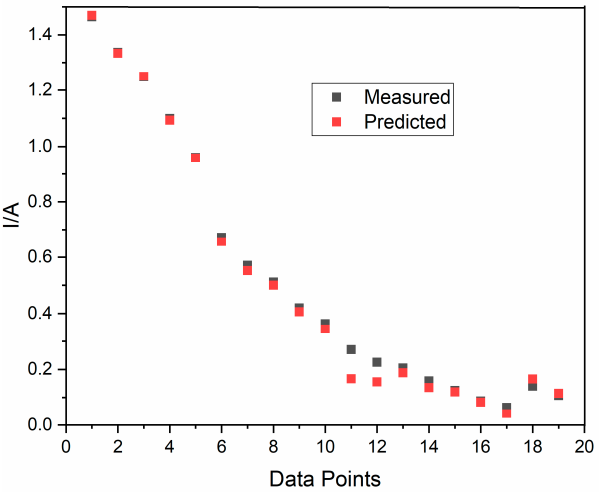

Figure 8. Results for measured and predicted current for training.

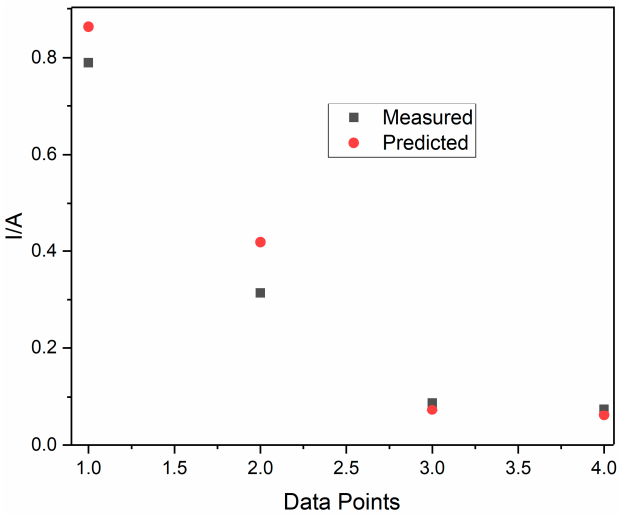

Figure 9. Results for measured and predicted current for testing.

Figures 10 and 11 also show the training and testing results obtained for voltage.

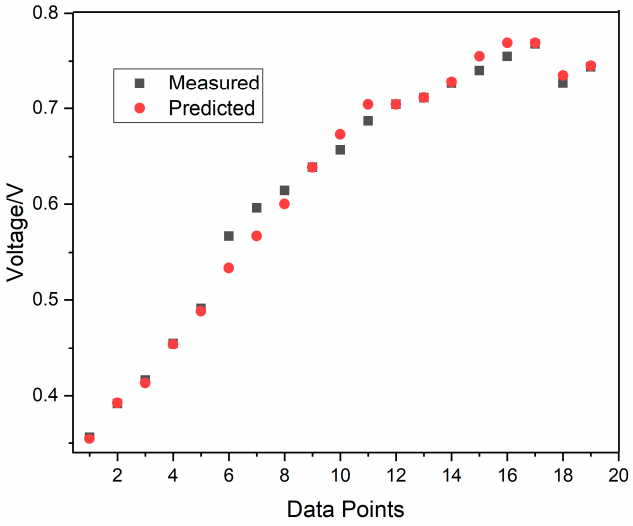

Figure 10. Results for measured and predicted voltage for training.

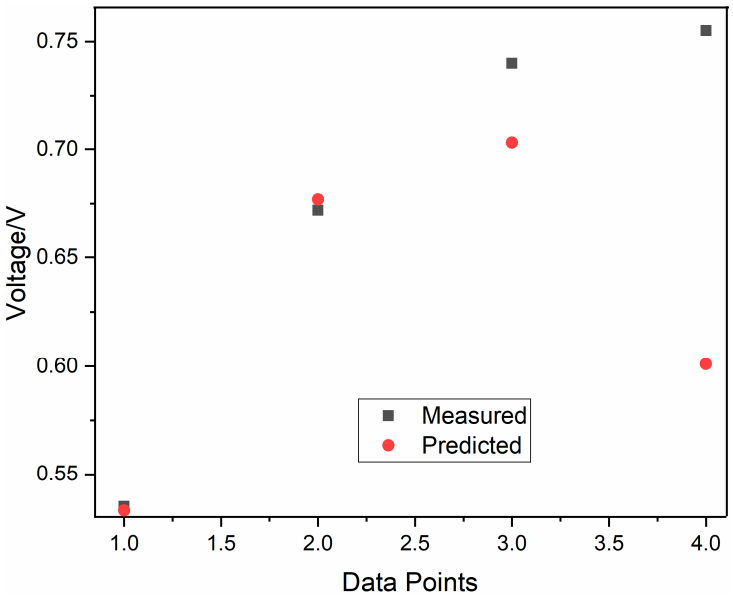

Figure 11. Results for measured and predicted voltage for testing.

The performance of the adaptive neuro-fuzzy inference system in the estimation of the current and voltage from the fuel cell experiment is evaluated. Table 8 captures the performance of the adaptive neuro-fuzzy inference model. Table 8 clearly shows that the RMSE value for the output parameters predicted were less than 1, indicating accurate results. In spite of the training for the current performing better compared to other models, there were no observable differences identified. The learning conducted for the current was more accurate compared to the other output parameters. The prediction for the voltage also exhibited very good results. In summary, the predicted values for the dependent variables were in good agreement with the actual (experimental) results perfectly. Taking R^2 into consideration, the model prediction for the current was slightly better compared to the voltage for both the training and the testing.

Table 8. Performance of ANFIS models.

	Training Time (s)		**RMSE**		**R^2**	
	Training	Testing	Training	Testing	Training	Testing
Current	8.04	8.32	0.028235	0.42473	0.99193	0.9998
voltage	9.92	8.620	0.006513	0.078608	0.99069	0.99958

4. Conclusions

This investigation explored the application of an adaptive neuro-fuzzy inference system as a prediction technique for fuel cell experimental data obtained under laboratory conditions. The adaptive neuro-fuzzy inference system is made up of both fuzzy inference and artificial neural network. This technique has been utilized in a number of research activities in applied science for predicting output variables knowing the independent variables. This research was aimed at predicting current and voltage based on experimental data from proton exchange membrane fuel cell at different operational conditions. The model was adopted after it was deduced that using the multiple linear regression led to the creation of non-linearities in the predicted results. Hydrogen flow rate and pressure were used as the independent variable. The experimental data were then trained and tested. The outcome of the results generated showed excellent results hence the potential for the application of adaptive neuro-fuzzy inference system in fuel cell statistical analysis and prediction. It was further deduced that due to the cost of producing hydrogen, a good balance between the pressure and flow rate would significantly reduce the cost of operation for the fuel cell. Furthermore, losses (pumping power,

mass concentration losses, and activation losses) in the PEM fuel cell are reduced significantly if the flowrates between the fuel and oxidant are carefully selected based on the application, as captured in this investigation.

Author Contributions: Data curation, T.W.; formal analysis, T.W. and A.G.O.; methodology, T.W.; project administration, A.G.O.; supervision, A.G.O. All authors have read and agreed to the published version of the manuscript.

Funding: This research received no external funding.

Conflicts of Interest: The authors declare no conflict of interest.

References

1. Nguyen, T.-T.; Fushinobu, K. Effect of operating conditions and geometric structure on the gas crossover in PEM fuel cell. *Sustain. Energy Technol. Assess.* **2020**, *37*, 100584. [CrossRef]
2. Baroutaji, A.; Wilberforce, T.; Ramadan, M.; Olabi, A.G. Comprehensive investigation on hydrogen and fuel cell technology in the aviation and aerospace sectors. *Renew. Sustain. Energy Rev.* **2019**, *106*, 31–40. [CrossRef]
3. Laribi, S.; Mammar, K.; Sahli, Y.; Koussa, K. Analysis and diagnosis of PEM fuel cell failure modes (flooding & drying) across the physical parameters of electrochemical impedance model: Using neural networks method. *Sustain. Energy Technol. Assess.* **2019**, *34*, 35–42.
4. Ijaodola, O.S.; Hassan, Z.E.; Ogungbemi, E.; Khatib, F.N.; Wilberforce, T.; Thompson, J.; Olabi, A.G. Energy efficiency improvements by investigating the water flooding management on proton exchange membrane fuel cell (PEMFC). *Energy* **2019**, *179*, 246–267. [CrossRef]
5. Sayed, E.T.; Eisa, T.; Mohamed, H.O.; Abdelkareem, M.A.; Allagui, A.; Alawadhi, H.; Chae, K.-J. Direct urea fuel cells: Challenges and opportunities. *J. Power Sources* **2019**, *417*, 159–175. [CrossRef]
6. Ogungbemi, E.; Ijaodola, O.; Khatib, F.N.; Wilberforce, T.; el Hassan, Z.; Thompson, J.; Ramadan, M.; Olabi, A.G. Fuel cell membranes—Pros and cons. *Energy* **2019**, *172*, 155–172. [CrossRef]
7. Priya, K.; Babu, T.S.; Balasubramanian, K.; Kumar, K.S.; Rajasekar, N. A novel approach for fuel cell parameter estimation using simple Genetic Algorithm. *Sustain. Energy Technol. Assess.* **2015**, *12*, 46–52. [CrossRef]
8. Khatib, F.N.; Wilberforce, T.; Ijaodola, O.; Ogungbemi, E.; El-Hassan, Z.; Durrant, A.; Thompson, J.; Olabi, A.G. Material degradation of components in polymer electrolyte membrane (PEM) electrolytic cell and mitigation mechanisms: A review. *Renew. Sustain. Energy Rev.* **2019**, *111*, 1–14. [CrossRef]
9. Thamer, B.M.; El-Newehy, M.H.; Barakat, N.A.; Abdelkareem, M.A.; Al-Deyab, S.S.; Kim, H.Y. In-situ synthesis of Ni/N-doped CNFs-supported graphite disk as effective immobilized catalyst for methanol electrooxidation. *Int. J. Hydrogen Energy* **2015**, *40*, 14845–14856. [CrossRef]
10. Marefati, M.; Mehrpooya, M. Introducing a hybrid photovoltaic solar, proton exchange membrane fuel cell and thermoelectric device system. *Sustain. Energy Technol. Assess.* **2019**, *36*, 100550. [CrossRef]
11. Abdelkareem, M.A.; al Haj, Y.; Alajami, M.; Alawadhi, H.; Barakat, N.A.M. Ni-Cd carbon nanofibers as an effective catalyst for urea fuel cell. *J. Environ. Chem. Eng.* **2018**, *6*, 332–337. [CrossRef]
12. Olabi, A.G.; Mahmoud, M.; Soudan, B.; Wilberforce, T.; Ramadan, M. Geothermal based hybrid energy systems, toward eco-friendly energy approaches. *Renew. Energy* **2020**, *147 Pt 1*, 2003–2012. [CrossRef]
13. Subin, K.; Jithesh, P.K. Experimental study on self-humidified operation in PEM fuel cells. *Sustain. Energy Technol. Assess.* **2018**, *27*, 17–22. [CrossRef]
14. Wilberforce, T.; Nisar, F.; Ogungbemi, E.; Olabi, A.G. Water Electrolysis Technology. *Ref. Module Mater. Sci. Mater. Eng.* **2018**. [CrossRef]
15. Heck, J.D.; Vaz, W.S.; Koylu, U.O.; Leu, M.C. Decoupling pressure and distribution effects of flow fields on polymer electrolyte fuel cell system performance. *Sustain. Energy Technol. Assess.* **2019**, *36*, 100551. [CrossRef]
16. Wilberforce, T.; El-Hassan, Z.; Khatib, F.N.; al Makky, A.; Baroutaji, A.; Carton, J.G.; Olabi, A.G. Developments of electric cars and fuel cell hydrogen electric cars. *Int. J. Hydrogen Energy* **2017**, *42*, 25695–25734. [CrossRef]
17. Wilberforce, T.; El-Hassan, Z.; Khatib, F.N.; al Makky, A.; Baroutaji, A.; Carton, J.G.; Mooney, J.; Olabi, A.G. Development of Bi-polar plate design of PEM fuel cell using CFD techniques. *Int. J. Hydrogen Energy* **2017**, *42*, 25663–25685. [CrossRef]

18. Thamer, B.M.; El-Newehy, M.H.; Barakat, N.A.; Abdelkareem, M.A.; Al-Deyab, S.S.; Kim, H.Y. Influence of nitrogen doping on the catalytic activity of Ni-incorporated carbon nanofibers for alkaline direct methanol fuel cells. *Electrochim. Acta* **2014**, *142*, 228–239. [CrossRef]
19. Ma, L.; Ingham, D.B.; Pourkashanian, M.; Carcadea, E. Review of computational dynamics modeling of fuel cells. *J. Fuel Cell Sci. Technol.* **2005**, *2*, 246–257. [CrossRef]
20. Haddad, A.; Bouyekhf, R.; Moudni, A.E. Dynamic modeling and water management in proton exchange membrane fuel cell. *Int. J. Hydrogen Energy* **2008**, *33*, 6239–6252. [CrossRef]
21. Sharma, M. Artificial neural network fuzzy inference system (ANFIS) for brain tumor detection. *arXiv* **2012**, arXiv:1212.0059.
22. Atuahene, S.; Bao, Y.; Ziggah, Y.; Gyan, P.; Li, F. Short-Term Electric Power Forecasting Using Dual-Stage Hierarchical Wavelet-Particle Swarm Optimization-Adaptive Neuro-Fuzzy Inference System PSO-ANFIS Approach Based on Climate Change. *Energies* **2018**, *11*, 2822. [CrossRef]
23. Ni, M.; Leung, D.Y.C.; Leung, M.K.H. Mathematical modeling of ammonia-fed solid oxide fuel cells with different electrolytes. *Int. J. Hydrogen Energy* **2008**, *33*, 5765–5772. [CrossRef]
24. Pramuanjaroenkij, A.; Kakac, S.; Zhou, X.Y. Mathematical analysis of planar solid oxide fuel cells. *Int. J. Hydrogen Energy* **2008**, *33*, 2547–2565. [CrossRef]
25. Rafiq, M.Y.; Bugmann, G.; Easterbrook, D.J. Neural network design for engineering applications. *Comput. Struct.* **2001**, *79*, 1541–1552. [CrossRef]
26. Gorzalczany, M.B. *Computational Intelligence Systems and Applications*; Physica: Heidelberg, Germany, 2002.
27. Arriagada, J.; Olausson, P.; Selimovic, A. Artificial neural network simulator for SOFC performance predictions. *J. Power Sources* **2002**, *112*, 54–60. [CrossRef]
28. Ou, S.; Achenie, L.E.K. A hybrid neural network model for PEM fuel cells. *J. Power Sources* **2005**, *140*, 319–330. [CrossRef]
29. Wu, X.J.; Zhu, X.J.; Cao, G.Y.; Tu, H.Y. Modelling a SOFC stack based on GA-RBF neural networks identification, networks identification. *J. Power Sources* **2007**, *167*, 145–150. [CrossRef]
30. Jurado, F. Predictive control of solid oxide fuel cells using fuzzy Hammerstein model. *J. Power Sources* **2006**, *158*, 245–253. [CrossRef]
31. Sun, T.; Yan, S.; Cao, G.; Zhu, X. Modeling and control PEMFC using fuzzy neural networks. *Zhejiang Univ.* **2005**, *10*, 1084–1089.
32. Entchev, E.; Yang, L. Application of adaptive neuro-fuzzy inference system techniques and artificial neural networks to predict solid oxide fuel cell performance in residential microgeneration installation. *J. Power Sources* **2007**, *170*, 122–129. [CrossRef]
33. Wang, R.; Qi, L.; Xie, X.; Ding, Q.; Li, C.; Ma, C.M. Modeling a 5-cell direct methanol fuel cell using adaptive-network based fuzzy inference systems. *J. Power Sources* **2008**, *185*, 1201–1208. [CrossRef]
34. Wu, X.; Zhu, X.; Cao, G.; Tu, H. Nonlinear modeling of a SOFC based on ANFIS identification. *Simul. Model. Pract. Theor.* **2008**, *16*, 399–409. [CrossRef]
35. Jang, J.S.R. ANFIS: Adaptive network-based fuzzy inference system. *IEEE Trans. Syst. Man Cybern.* **1993**, *23*, 665–685. [CrossRef]
36. Jang, J.S.R.; Sun, C.T. Neuro-fuzzy modeling and control. *Proc. IEEE* **1995**, *83*, 378–406. [CrossRef]
37. *Fuzzy Logic. Toolbox User's Guide*; Version 2; The MathWorks, Inc.: Natick, MA, USA, 2001; Available online: https://www.tandfonline.com/toc/tfie20/current?gclid=CjwKCAjw26H3BRB2EiwAy32zhfLMQsHzBOxi7pKRErCr9LUq2cmn5dU5_jTDjL5EVxRSdac9iZoVeBoCrFkQAvD_BwE (accessed on 16 June 2020).
38. Wang, L.; Husar, A.; Xhou, T.Z.; Liu, H. A parametric study of PEM fuel cell performances. *Int. J. Hydrogen Energy* **2003**, *28*, 1263–1272. [CrossRef]
39. Jang, J.S.R. Input selection for ANFIS Learning. In Proceedings of the IEEE 5th International Fuzzy Systems, New Orleans, LA, USA, 11 September 1996.